ORIGINAL ARTICLE

Morphologic Characterization of Nerves in Whole-Mount Airway Biopsies

Peter W. West[1], Brendan J. Canning[2], Emilio Merlo-Pich[3], Ashley A. Woodcock[1], and Jaclyn A. Smith[1]

[1]Centre for Respiratory Medicine and Allergy, Faculty of Medical and Human Sciences, University of Manchester, Manchester, United Kingdom; [2]Division of Allergy and Clinical Immunology, Department of Medicine, Johns Hopkins Asthma and Allergy Center, Baltimore, Maryland; and [3]Takeda Pharmaceuticals, High Wycombe, United Kingdom

ORCID ID: 0000-0001-8837-4928 (J.A.S.).

Abstract

Rationale: Neuroplasticity of bronchopulmonary afferent neurons that respond to mechanical and chemical stimuli may sensitize the cough reflex. Afferent drive in cough is carried by the vagus nerve, and vagal afferent nerve terminals have been well defined in animals. Yet, both unmyelinated C fibers and particularly the morphologically distinct, myelinated, nodose-derived mechanoreceptors described in animals are poorly characterized in humans. To date there are no distinctive molecular markers or detailed morphologies available for human bronchopulmonary afferent nerves.

Objectives: Morphologic and neuromolecular characterization of the afferent nerves that are potentially involved in cough in humans.

Methods: A whole-mount immunofluorescence approach, rarely used in human lung tissue, was used with antibodies specific to protein gene product 9.5 (PGP9.5) and, for the first time in human lung tissue, 200-kD neurofilament subunit.

Measurements and Main Results: We have developed a robust technique to visualize fibers consistent with autonomic and C fibers and pulmonary neuroendocrine cells. A group of morphologically distinct, 200-kD neurofilament-immunopositive myelinated afferent fibers, a subpopulation of which did not express PGP9.5, was also identified.

Conclusions: PGP9.5-immunonegative nerves are strikingly similar to myelinated airway afferents, the cough receptor, and smooth muscle–associated airway receptors described in rodents. These have never been described in humans. Full description of human airway nerves is critical to the translation of animal studies to the clinical setting.

Keywords: afferent neurons; mechanoreceptors; peripheral nervous system; lung

At a Glance Commentary

Scientific Knowledge on the Subject: The cough reflex is mediated by vagal afferent nerves in humans, and the responsible A-delta and C-fiber nerves have been well described in animals. We describe innervation in human airways with novel morphology similar to vagal afferents described in animals.

What This Study Adds to the Field: This is the first study to describe the potential vagal afferents responsible for cough in human airways. This level of detail has never before been described, yet it is vital for the effective development of treatments for neural targets in the lungs.

The role of airway innervation in respiratory disease has received little attention in recent years, despite the clear involvement of neuronal pathways in respiratory symptoms, such as dyspnea, wheeze, bronchoconstriction, mucus hypersecretion, and cough (1), characteristics of many respiratory diseases that impact significantly on patients' quality of life (2). Patients suffering from chronic cough describe enhanced sensitivity to a variety of inhaled irritants and air

(Received in original form December 23, 2014; accepted in final form April 3, 2015)

Supported by funds from the National Institute of Health Research clinical research facility and University Hospital of South Manchester endowment fund. J.A.S. has received a Medical Research Council clinician scientist award. P.W.W. received a travel grant from the British Society for Immunology for a laboratory visit to Johns Hopkins University, which facilitated this collaboration.

Author Contributions: Study concept and design, all authors. Acquisition of samples and data, P.W.W., A.A.W., and J.A.S. Drafting of the manuscript, P.W.W., B.J.C., and J.A.S. Critical revision of manuscript, all authors. Statistical analysis, P.W.W. and J.A.S. Obtained funding, A.A.W., J.A.S., and P.W.W. P.W.W. and J.A.S. had full access to all the data in the study and take responsibility for the integrity of the data and the accuracy of the data analysis.

Correspondence and requests for reprints should be addressed to Peter W. West, Ph.D., Centre for Respiratory Medicine and Allergy, 2nd Floor Education and Research Centre, University Hospital of South Manchester, Southmoor Road, Manchester M23 9LT, UK. E-mail: peter.west@manchester.ac.uk

This article has an online supplement, which is accessible from this issue's table of contents at www.atsjournals.org

Am J Respir Crit Care Med Vol 192, Iss 1, pp 30–39, Jul 1, 2015

Originally Published in Press as DOI: 10.1164/rccm.201412-2293OC on April 23, 2015
Internet address: www.atsjournals.org

temperature changes (3). In keeping with patient-reported symptoms, they also cough more readily in response to inhaled capsaicin or citric acid (4). This hypersensitivity may be caused by neuroplasticity in mucosal fibers, contributing to increased excitability of the afferent limb of the cough reflex (5).

Afferent fibers including those activated during breathing, such as slowly adapting receptors, rapidly adapting receptors, and those that mediate tussive responses to mechanical and chemical stimulation, broadly divided into rapidly transmitting A delta and slower C fibers, have been well defined in animals (6–9). Yet, prominent discoveries of immunochemically distinct receptor end organs, such as the unmistakable guinea pig cough receptor (10) and the murine smooth muscle–associated airway receptor and neuroepithelial body (NEB) innervation (11), have been conspicuously absent in descriptions of human airway innervation to date (12). The sparsity of such vagal afferent mechanoreceptors in comparison with the easily identified vagal and spinal C fiber counterparts and lack of appropriate antibodies might explain this phenomenon. However, it is also evident from published data and denervation studies that the immunologic markers, or the nerves themselves, decay rapidly in explanted tissue (13–15).

Few studies have used a whole-mount technique necessary for full morphologic description of human bronchopulmonary nerves, even fewer in whole-mount endobronchial biopsies (16, 17). Studies conducted to date are limited by the extent of innervation observed and antibodies used. In two studies that assessed epithelial nerves, the observed density was very low, in the range of 1–3% epithelial area (5, 18). In our experience, it is difficult to observe nerves in thin tissue sections and the frequent absence of innervation in published data suggests that it becomes even harder when targeting mainly C fiber–specific markers (5, 18). A detailed understanding of the afferent neuronal structures of the human airway, the presence of key ion channels and G-protein–coupled receptors at their terminals, and how these factors change in disease is central to the effective development of treatments of respiratory disorders associated with neural sensitization (5).

We capitalized on the opportunity to study endobronchial biopsies from a well-phenotyped group of patients with treatment-resistant chronic cough, who were undergoing clinical investigation and agreed to participate in the study. Here, we describe the extensive assessment of the innervation present in mucosal biopsy tissue and for the first time, morphologic equivalents of the innervation described in other species. Some of these results have previously been reported in abstract form (19, 20).

Methods

For detailed discussion of methods, *see* the online supplement.

Study Design, Samples, and Subjects

Study samples consisted of endobronchial biopsies obtained from 21 patients undergoing clinical bronchoscopy for a chronic cough (>8-wk duration). All subjects were attending a specialist cough clinic at University Hospital of South Manchester, United Kingdom and were enrolled in the ManRAB biobank (REC Ref: 10/H1010/7) between March 2011 and March 2012. All provided written informed consent. Characteristics of patients from whom data in this manuscript were obtained are shown in Table 1. Ex-smokers had at least a 9-year abstinence from smoking.

Bronchoscopy

Fiberoptic bronchoscopy was performed under conscious sedation with topical lidocaine. Endobronchial biopsies were obtained from the distal and proximal spurs of the right middle and lower lobes.

Immunofluorescence Microscopy Imaging

Briefly, biopsies were removed from the forceps into warmed (37°C) 0.9% sterile normal saline solution before immediate fixation in ice cold, 4% paraformaldehyde in Dulbecco phosphate-buffered saline solution containing protease inhibitors for 3 hours at 4°C. All subsequent incubations were performed at 4°C. Nonspecific binding was blocked using 10% normal serum, 1% skimmed milk, and 0.5% Triton X-100 for tissue permeabilization. Immunofluorescent staining was performed using specific primary antibodies and Alexa Fluor–labeled secondary antibodies (*see* Table E1 in the online supplement). Biopsies were mounted onto glass slides with coverslips. Images were collected using epifluorescence or confocal microscopy and adjusted as described in the online supplement. Where multiple fluorophores are shown, images were collected sequentially. Single-channel images are shown in the online supplement. Control experiments were performed by omitting primary antibody from the procedure. No immunoreactivity was observed in control biopsies.

A full list of antibodies trialed is detailed in the online supplement (*see* Table E1) but these data pertain to observations with anti–200-kD neurofilament (Leica Biosystems, Newcastle upon Tyne, UK) and anti–protein gene product 9.5 (PGP9.5; Ultraclone, Wellow, UK). The conventional use of these antibodies is to identify myelinated neurons, and as a panneuronal marker, respectively.

Table 1. Study Subject Characteristics

	All Patients
Number	21
Age, yr, mean (SEM)	58.9 (1.68)
Male, n (%)	8 (38.1)
Cough duration, yr, median (IQR)	8 (2.28–16)
Smoking status	
Never, n (%)	11 (52)
Ex-smoker, n (%)	10 (48)
Pack-years, n = 10, median (IQR)	9.5 (3.5–24)
Years since quit, median (IQR)	32 (21.5–37.25)
FEV_1, % predicted, mean (SEM)	113 (4.36)
FVC, % predicted, mean (SEM)	119 (3.81)

Definition of abbreviation: IQR = interquartile range.

Nerve Fiber Diameter Analysis

Nerve fiber diameter measurements were conducted on epifluorescence photomicrographs by a single observer. A mean of 2.5 fields per biopsy was chosen and a mean of 2.4 individual nonconnected nerve fibers per field was analyzed. Fiber diameters were based on an average of 24 manual linear measurements across each fiber, spaced at regular intervals of approximately 2–5 μm along its length.

Nerve Tracing

Computerized line drawings of nerves were produced from models, which were generated using Neuromantic version 1.7.5 (University of Reading, Reading, UK). Semiautomatic tracing was performed on grayscale conversions of original two-dimensional images. Plan view of the skeletonized model is presented as a guide to the structure observed.

Statistical Analysis

Data are expressed as median (interquartile range [IQR], 25th–75th percentile). Statistical comparisons were conducted on nonparametric data using the Mann-Whitney *U* test or Kruskal-Wallis test with Dunn's post-test correction in Prism Version 5 (Graphpad, San Diego, CA). Significant differences are presented as *P* less than 0.001.

Results

The results we present are primarily restricted to morphologic observations using antibodies immunoreactive to the structural proteins PGP9.5 and 200-kD neurofilament. Tissue was orientated with the epithelium uppermost and nerve fibers were identified by their associated structures, depth from the epithelium, and on the basis of published literature. We concentrated on structures within the epithelium and lamina propria, which studies suggest are more relevant to airway sensation (21, 22). We have only briefly described our observations of autonomic fibers and deeper neural plexuses because there is an extensive body of literature concerning human autonomic bronchopulmonary neurons.

Putative Autonomic Fibers

Fibers observed close to blood vessels, mucosal glands, and smooth muscle were presumed to be autonomic based on immunoreactivity to vesicular acetylcholine transporter and synaptic vesicle protein 2 and the known function of fibers in these locations. We observed two distinct subepithelial fiber types. One type was straighter and less branched than other observed fibers (Figure 1A) with a median (IQR) diameter of 1.44 (1.23–1.71) μm. α-Smooth muscle actin immunofluorescence revealed innervation of subepithelial blood vessels (Figure 1B; *see* Figures E2 and E3). These nerve fibers and blood

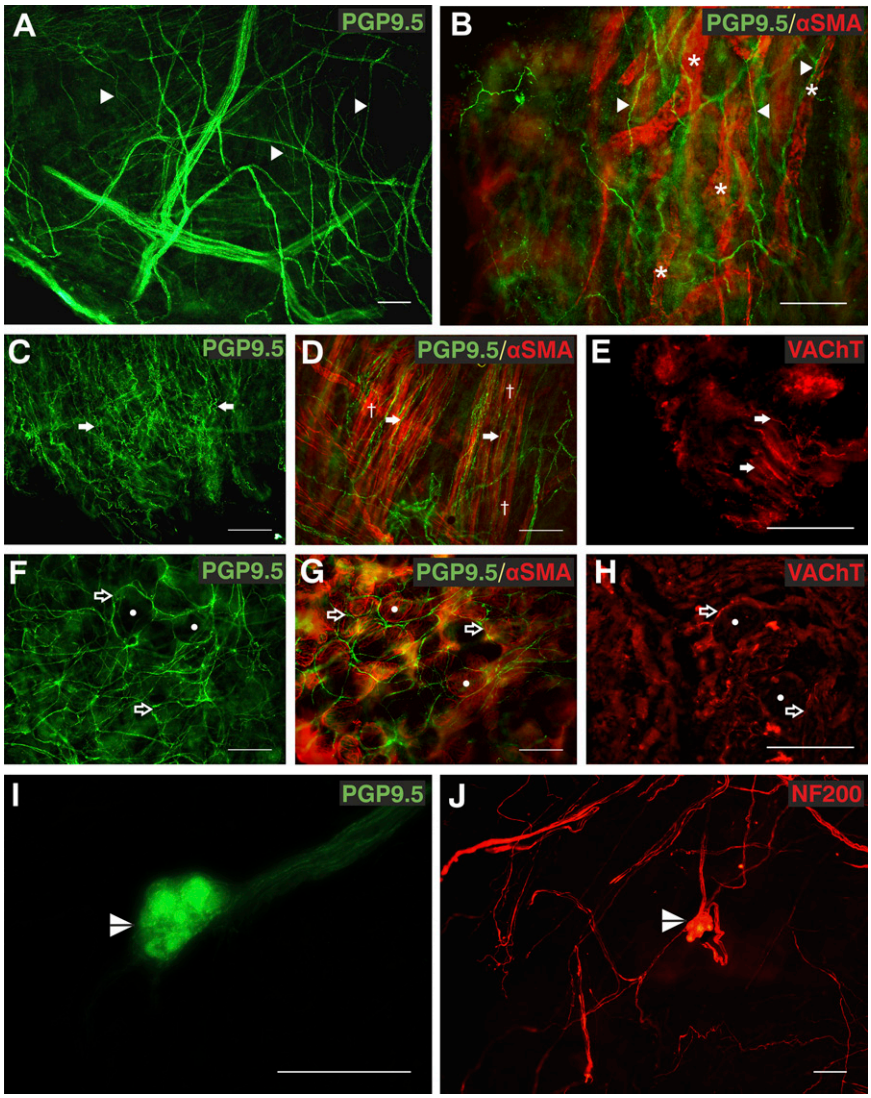

Figure 1. Autonomic fibers in the human airway mucosa. (*A* and *B*) Protein gene product 9.5 (PGP9.5) immunopositive (*green*, Alexa Fluor 488) subepithelial fibers (*arrowheads*) were associated with α-smooth muscle actin (SMA)-immunoreactive (*red*, Alexa Fluor 568) blood vessels (*asterisks*). (*C–E*) PGP9.5-immunopositive (*green*, Alexa Fluor 488) convoluted fibers (*arrows*) were observed in parallel to bronchial smooth muscle (*daggers*) labeled with α-SMA (*red*, Alexa Fluor 568) and a proportion were immunopositive for vesicular acetylcholine transporter (VAChT) (*red*, Alexa Fluor 568). (*F–H*) The distinctive circular pattern of PGP9.5 and VAChT immunoreactive fibers (*open arrows*) around acinar cells of bronchial mucosal glands observed with α-SMA (*circles*). (*I* and *J*) Airway intrinsic autonomic ganglia (*split arrowheads*) immunoreactive for both PGP9.5 (*green*, Alexa Fluor 488) and 200-kD neurofilament (NF200; *red*, Alexa Fluor 568) were observed. Biopsies were from right middle lobe entrance (*A*, *B*, *E*, *F*, and *H*), right lower lobe (*C*, *D*, and *G*), right upper lobe entrance (*I*), and right main bronchus (*J*). Results are independent experiments of staining in nine biopsies from seven patients. *Scale bars* = 100 μm. Unprocessed and single-channel images are shown in Figures E1 and E2 with additional images in Figure E3. A video of additional images of separate focal planes from *B* is shown in Video E1.

Table 2. Features Observed in Cough Patient Biopsies with PGP9.5 and 200-kD Neurofilament Immunofluorescence

Features Observed	Number of Biopsies Observed in PGP9.5 Positivity		Number of Biopsies Observed in 200-kD Neurofilament	
	Biopsies	Patients	Biopsies	Patients
Totals	38	20	19	11
Varicose epithelial fibers	25/38	16/20	8/19	7/11
Subepithelial fibers	36/38	20/20	17/19	10/11
Convoluted fibers	34/38	20/20	15/19	10/11
Mucosal gland innervation	22/38	16/20	6/19	5/11
Nerve trunks	38/38	20/20	17/19	10/11
PNEC	25/38	16/20	0/19	0/11
Morphologic afferents	4/38	3/20	7/19	7/11

Definition of abbreviations: PGP9.5 = protein gene product 9.5; PNEC = pulmonary neuroendocrine cells.

vessels were situated in the lamina propria between the epithelium and the smooth muscle layer. The second, deeper plexus comprised slightly thicker fibers with a median (IQR) diameter of 1.81 (1.50–2.17) μm, which we termed convoluted fibers. These fibers were observed within the smooth muscle layer (Figures 1C–1E) and also between this layer and the straighter fibers in the submucosa.

We observed distinctive circular patterns of PGP9.5-positive nerves (Figure 1F), consistent with fibers underlying the basal membrane of the serous acini of submucosal glands in 58% of biopsies. α-Smooth muscle actin and cytokeratin staining confirmed this observation, allowing visualization of the tubules and myoepithelial cells of the gland (Figure 1G; *see* Figures E1–E3). Mucosal gland fibers had a median (IQR) diameter of 1.97 (1.65–2.41) μm. We observed airway ganglia in five biopsies. These were both PGP9.5 and 200-kD neurofilament immunopositive (Figures 1I and 1J). Four of the ganglia were small in size (median [IQR], 53.5 [36] × 88 [47.25] μm) and were closely associated with airway smooth muscle. One larger ganglion was 175 × 240 μm.

Convoluted and mucosal fibers expressed the vesicular acetylcholine transporter, a marker of cholinergic nerves (Figures 1E and 1H) (23). Both subepithelial fiber types were observed in biopsies from all sampling locations in all 20 patients where biopsies were stained for PGP9.5. Mucosal glands were observed in PGP9.5-stained biopsies from 16 out of 20 patients and in all sampled regions (Table 2), but only in 1 of 15 biopsies taken from the right main stem bronchus (total eight subjects). Additional images are shown in Figures E1–E3 and Video E1.

Varicose Epithelial Fibers and Pulmonary Neuroendocrine Cells

We observed the presence of fine, varicose epithelial nerves and pulmonary

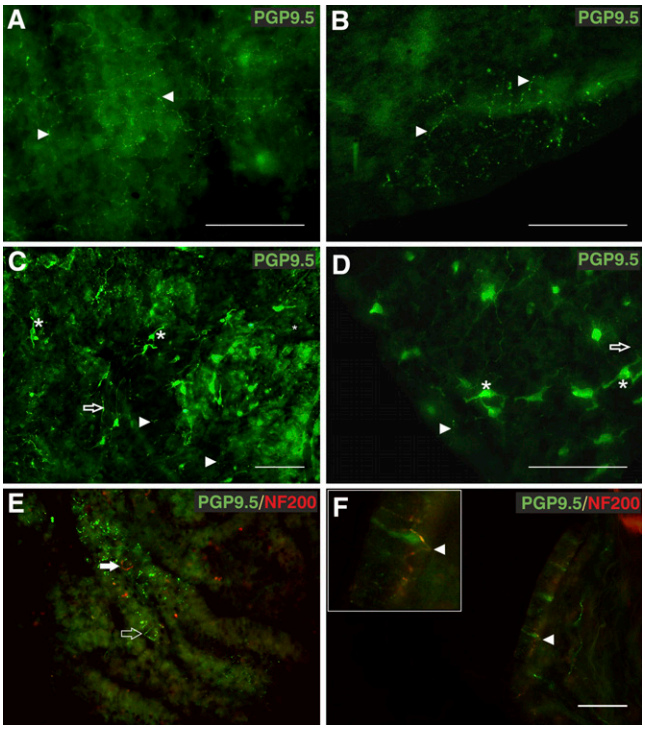

Figure 2. Protein gene product 9.5 (PGP9.5) immunoreactivity in human airway epithelium. (*A* and *B*) PGP9.5-immunopositive (*green*, Alexa Fluor 488) varicose epithelial fibers (*arrowheads*) appeared in patches at the luminal edge of the epithelium. (*C* and *D*) A population of epithelial cells were immunoreactive for PGP9.5, with typical flask-shaped pulmonary neuroendocrine cell morphology (*asterisks*) and cellular projections (*open arrows*). Segments of epithelial fibers were also observed (*arrowheads*). (*E* and *F*) Epithelial fibers were mostly 200-kD neurofilament (NF200) immunonegative (*open arrow*), but some were observed only with antineurofilament (*red*, Alexa Fluor 568, *solid arrow*) or were dual positive (*arrowheads*). Biopsies were from right main bronchus (*A*, *D*, and *E*) and right middle lobe entrance (*B*, *C*, and *F*). Results shown are independent experiments of six biopsies from separate patients. *Scale bars* = 100 μm. Unprocessed, single-channel images, additional images, and videos are shown in Figures E4–E6 and Videos E2 and E3.

neuroendocrine cells (PNECs) in biopsies from 16 of the 20 patients whose tissue was stained for PGP9.5 (Table 2). These biopsies were from the basal segments of the right lower lobe, the right middle lobe entrance, right upper lobe entrance, and right main stem bronchus. These fibers formed extensively branched networks across the epithelium (Figures 2A and 2B; *see* Figure E6) and occurred in patches of variable size (~50–500 μm). A median (IQR) of 33.3% (25.4%) of these fibers were concurrent with areas of PNECs. We observed solitary PGP9.5-positive PNECs (Figures 2C and 2D) in three patients; in all other cases PNECs were observed in clusters, but not NEBs. The number of PNECs in these clusters ranged from 10 to greater than 100 (*see* Figure E6 and Videos E2 and E3). We calculated, from counting the number of cells per target area (area range varied from 4 to 16×10^4 μm^2) on photomicrographs, that PGP9.5-immunoreactive cells occur at a mean density of 267 (168–375) cells per square millimeter, accounting for 0.2–1.2% of epithelial cells in these areas. PGP9.5-immunopositive varicose fibers were associated with a median (IQR) of 70.8% (63.5%) of PNECs clusters.

Although the epithelial fibers were predominantly PGP9.5 immunopositive, small numbers of them were immunoreactive to anti–200-kD neurofilament or were dual positive (Figures 2E and 2F; *see* Figure E5).

Fiber Diameter Analysis

Measured nerve fibers from PGP9.5-immunostained biopsies were grouped morphologically (Figure 3). Epithelial nerves had a significantly smaller median (IQR) diameter (0.73 [0.68–0.84] μm) than other nerve types, and nerve bundles with a median (IQR) diameter of 16.12 (10.40–25.51) μm were significantly larger than all other nerve fibers. Other fiber subtypes were not significantly different (Kruskal-Wallis test with Dunn's post-test correction). Smoking history had no significant effect on the diameter of any fiber type (Mann-Whitney *U* test).

Potential Afferent Neurons

Based on the assumption that fibers within the epithelium likely responded to the luminal environment, we observed these fibers in more detail. Some epithelial fibers arose from thicker subepithelial fibers that branched extensively at the basement membrane just below the epithelium, with fine projections throughout the epithelial layer (Figure 4A; *see* Video E4). For others, no obvious origin could be ascribed, although epithelial projections were apparently derived from a shallower plexus of nerves (Figure 4B; *see* Video E4) and seemingly consisted of directionally parallel fibers arising from the subepithelial plexus and anastomosing at many points in the epithelial plexus to form an interconnected network (*see* Figure E9). PNECs and blood vessels were more common in these areas. Other epithelial fiber patches seemed to arise directly from nerve trunks, branching within the epithelial plexus (Figure 4C). We noted the arboreal appearance of some fibers and used DAPI (4′,6-diamidino-2-phenylindole) to confirm that these structures were innervating the epithelium (Figure 4D; *see* Figure E8). These fibers branched extensively from a single point and at least a proportion were 200-kD neurofilament immunopositive in the thicker parts of the fiber, whereas varicosities were only detected with PGP9.5 immunofluorescence (Figures 4F–4H). In all cases, epithelial fibers formed discrete areas, presumably receptive fields.

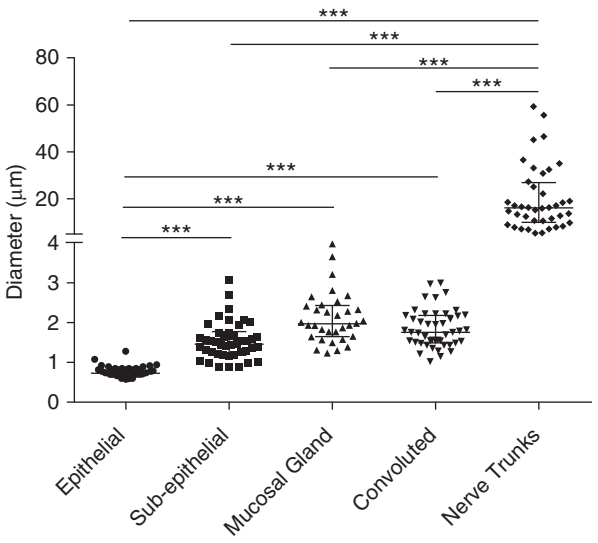

Figure 3. Nerve fiber diameter analysis. The median fiber diameter (in micrometers) of five identified protein gene product 9.5–stained fiber subtypes is shown. Measurements (n = 200 fibers) were obtained from 31 biopsies of 18 patients and grouped morphometrically into epithelial (n = 35), subepithelial (n = 42), mucosal gland (n = 32), convoluted (n = 44), and nerve trunk (n = 40). Individual fiber diameters are represented as separate data points, with *midline* and *error bars* to indicate median diameters with interquartile range. ***Significant differences ($P < 0.001$, Kruskal-Wallis test with Dunn's post-test correction).

PGP9.5-Immunonegative fibers

Some arboreal fibers were only identifiable when labeled with 200-kD neurofilament (Figure 5; *see* Figures E10–E12 and Video E5). These nerves were commonly located beneath the epithelium and were laterally branched with terminal buds. These fibers were thicker than PGP9.5-immunopositive fibers with diameters of 3–6 μm, consistent with thinly myelinated fibers that conduct in the A delta range. The morphology of these fibers shows similarity to subsets of neurofilament-positive airway afferents identified in animals, such as the "cough receptors." Of note, there was little PGP9.5 positivity in the region of these receptors, with the exception of one receptor (Figure 5C), which seemed to terminate in contact with PGP9.5-positive PNECs. This finding was a unique observation because this PGP9.5-negative fiber branched at the epithelium rather than in the region of the basement membrane but yet was not morphologically similar to other epithelial fibers.

Antibodies to Further Markers

Despite extensive trials, we were unable to detect any specific staining of the sort observed with PGP9.5 or 200-kD neurofilament in this tissue, with

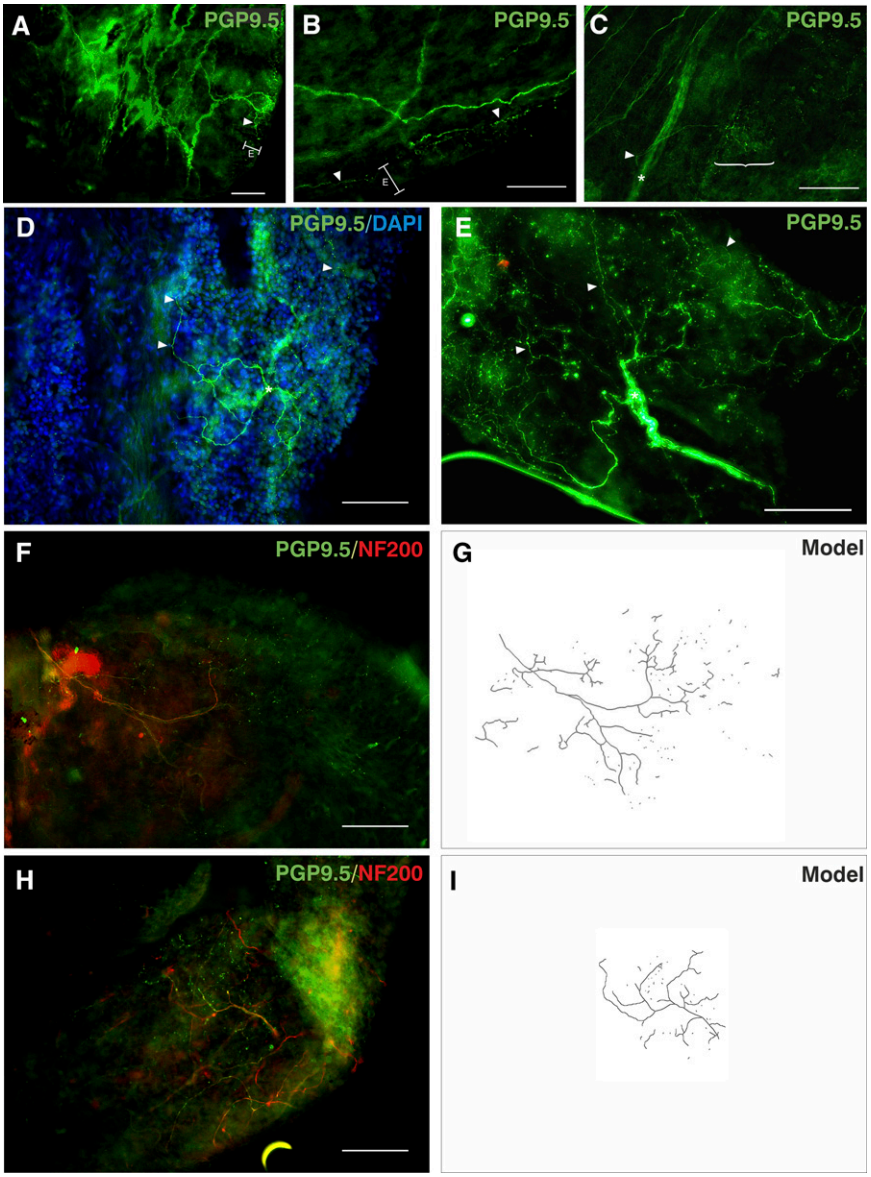

Figure 4. Protein gene product 9.5 (PGP9.5)-immunoreactive putative airway afferent fibers. Immunostaining for PGP9.5 (*green*, Alexa Fluor 488) 200-kD neurofilament (NF200; *red*, Alexa Fluor 568) using 4′,6-diamidino-2-phenylindole (DAPI; *blue*) as a nuclear counterstain (where shown). (*A* and *B*) Nerves that gave rise to varicosities in the epithelial plexus (E) were associated with nerve branches located superficially near the epithelial basement membrane (*arrowheads*). (*C*) Some similar-sized axons (*arrowhead*), which gave rise to epithelial fibers (*bracket*), arose directly from deeper nerve trunks (*asterisk*). (*D* and *E*) Varicose epithelial fibers (*arrowheads*) were arranged into extensively branched arboreal structures from a central point (*asterisks*). (*F–I*) The main branches of these fibers were immunopositive for NF200, whereas varicose nerve endings were only immunopositive for PGP9.5. (*G* and *I*) Computerized tracings show that these fibers form part of a larger arboreal structure, which appeared partly fragmented. Data are from biopsies from right middle lobe entrance (*A–C* and *H*); right lower lobe (*D* and *E*); and right main bronchus (*F*) from six separate patients. *E* is a maximum-intensity projection of five epifluorescent images. *Scale bars* = 100 μm. Unprocessed, single-channel, and additional images are shown in Figures E7 and E8 and Video E4.

antibodies directed against α3 subunit of Na^+/K^+-ATPase, transient receptor potential cation channel (TRP) vanilloid 1 and 4, TRP melastatin 8, TRP ankyrin 1, acid-sensing ion channel 3, and brain-derived neurotrophic factor, as previously described in animals. We identified extensive neuronal processes with an antibody to the βIII-tubulin subunit and some staining was also observed with antibodies directed to substance P, neuron-specific enolase, and synaptic vesicle protein (data not shown).

Discussion

Very few studies have used a whole-mount approach to investigate neuronal structures in human airways. This approach provides a significant improvement on traditional sectioning and staining techniques. It enables greater preservation and provides easier identification of the neuronal structures in three dimensions, which would otherwise be difficult to detect. Using this technique has allowed us to reveal morphologic structures akin to airway afferent nerves, such as cough receptors, which have not previously been described in human tissue.

Methodologic Approach

Despite work that has described the innervation of segments of the bronchial mucosa over a period of many decades, the picture of airway mucosal innervation in humans is still to be fully elucidated in a manner similar to that conducted in animals (24). There are several ways in which structure and function of airway nerves have been determined in animals, many of them powerful, but invasive (6, 14, 25). These techniques are not available for use in humans and so development of robust antibody techniques and careful characterization is paramount for the translation of animal data into the clinical setting. Therefore we have developed a robust procedure for the identification of airway nerves in patient samples. As others have described (24), immediate fixation in fresh fixative was paramount, particularly for the preservation of epithelial fibers. Corresponding to this observation, much longer timeframes before downstream processing were detrimental to our results. This may account for the paucity of epithelial nerves described in similar human studies (26).

Although previous studies examining epithelial nerve density have suggested sensitization of epithelial C fibers in patients with chronic cough, it was not the aim of this study to

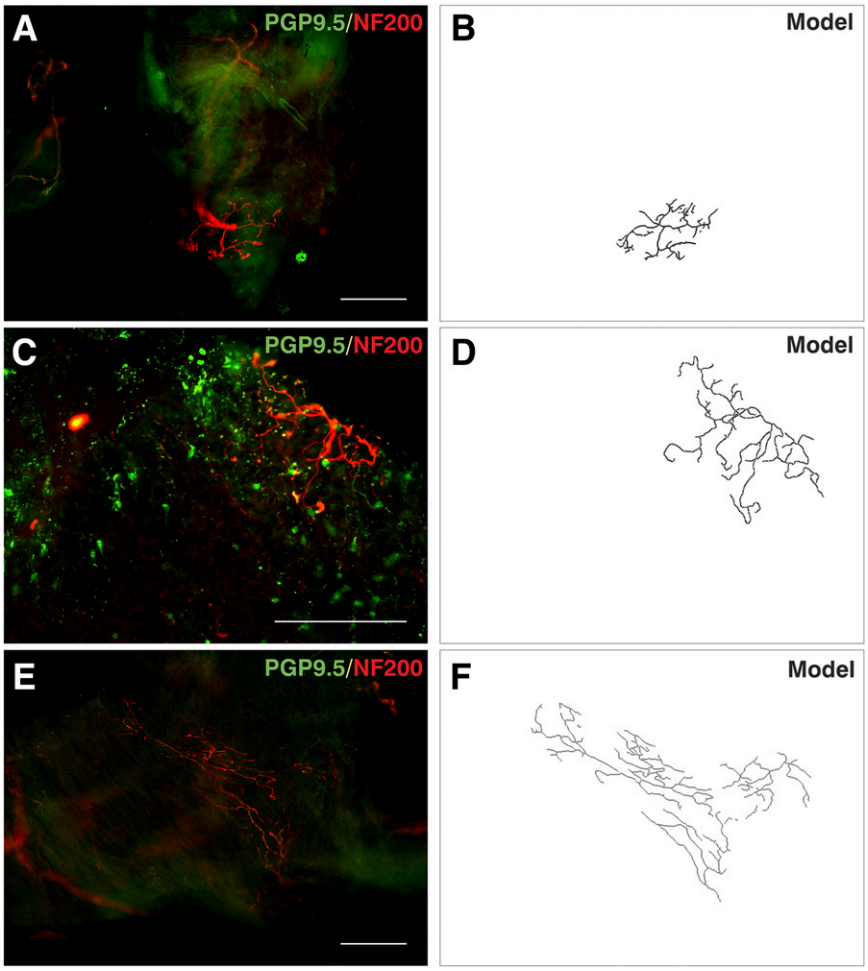

Figure 5. Protein gene product 9.5 (PGP9.5)-immunonegative afferent fibers. Tissue was observed using PGP9.5 (*green*, Alexa Fluor 488) and 200-kD neurofilament (NF200; *red*, Alexa Fluor 568) immunofluroescence. (*A*, *C*, and *E*) Neuronal structures were observed that were PGP9.5 negative but NF200 positive. There were fewer other neuronal structures in these regions, but successful PGP9.5 immunostaining identified neurons and pulmonary neuroendocrine cells (*A* and *C*). Pulmonary neuroendocrine cells were observed in close association with terminals of a thick NF200-stained nerve. (*B*, *D*, and *F*) Computerized grayscale tracings show the outline structure of fibers. Data are from three biopsies from the right middle lobe entrance (*A* and *C*) and right main bronchus (*E*) of three separate subjects. *Scale bars* = 200 μm. Unprocessed, single-channel, and additional images are shown in Figures E9–E11 and Video E5.

compare patient groups (18). Therefore we cannot know whether the types of neuronal structures described in this study would differ from those in healthy volunteers. However, we speculate that using tissue from patients may increase the likelihood of detecting neuronal structures.

In animals, often whole explanted airways can be observed, whereas we were only able to gain small samples from the airway mucosa of our patients. Structures present in other pulmonary locations were not identified by this approach. Nonetheless, we have elucidated many of the features, particularly autonomic fibers, which have previously been observed in larger samples, which validates our approach. Although the morphologic equivalents of cough receptors have been located mainly in the trachea and main bronchi of rodents (27), further observations suggest that airway afferent fibers including mechanoreceptors can be observed around the bifurcations in the lobar bronchi (13, 28, 29) where cough receptors are best placed to respond to insults. Sampling at carina is a standard practice for airway biopsy and so this would have increased our chances of detecting mechanosensitive airway fibers.

Observations

Without the ability to trace and analyze the cell bodies, it is difficult to draw robust conclusions about the origin of fibers, be they afferent or efferent. We have made inferences based on location, morphology, and size in combination with data drawn from animals to describe the innervation we observed (Figure 6). We concluded that fibers within smooth muscle bundles, surrounding mucosal glands, and parallel to blood vessels were likely autonomic fibers. Their known function in controlling mucus secretion, bronchoconstriction, and edema as well as their similar size (~1.5–2 μm) makes this the most likely explanation and is consistent with our observations of vesicular acetylcholine transporter immunofluorescence, mostly smaller nerve trunks (<20 μm) and the presence of small ganglia (14, 30, 31).

Afferent fibers may also be in these locations but our methods would not have been able to differentiate them (32). The neuropeptide content of some fibers may support a hypothesis of sensory innervation and shared vagal origin for a proportion of these fibers (14, 29). However, parasympathetic autonomic fibers can also express neuropeptides (33). Despite clear functional separation it is not yet apparent which markers might easily distinguish afferent from efferent innervation within human lung tissue. This issue is complicated by the poor cross-reactivity of antibodies, which are effective in animals.

Previous studies have shown that about 85% of fibers innervating the lung from the vagus nerve are pulmonary afferents (34) and so there is good reason to believe that we have identified afferent fibers. It is widely believed that the terminal varicosities of epithelial fibers are nociceptive C fibers based mainly on observations in animals that they express neuropeptides, such as calcitonin gene-related peptide, and can be traced to vagal sensory ganglia (21). Fiber diameters of less than 1 μm are consistent with this belief but we have been unable to obtain convincing classical C fiber

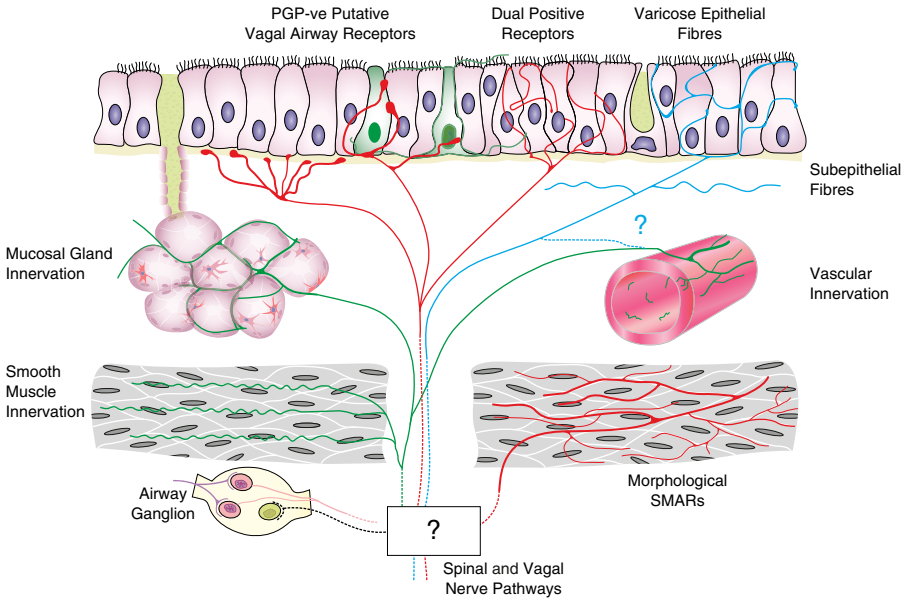

Figure 6. Schematic representation of the putative innervation of human airway mucosa based on morphologic observations from this study. Areas that are unknown or unproved are notated by a *question mark*. Airway ganglia and protein gene product 9.5 (PGP9.5)-immunopositive innervation of mucosal glands, smooth muscle, and mucosal blood vessels was observed. Putative afferent epithelial fibers with multiple morphologies may represent separate types. PGP9.5-immunonegative (PGP-ve) putative vagal afferents and morphologic equivalents of rodent vagal afferent receptors were identified with antibodies to 200-kD neurofilament. Varicose epithelial fibers have morphology and diameters consistent with C fibers. Neurofilament-immunopositive fine epithelial fibers may be the terminals of myelinated afferents. SMAR = smooth muscle–associated airway receptor.

immunolabeling patterns of these fibers, which may reflect the antibodies trialed. However, it is not clear that the expression of these labels is universal in all human epithelial fibers (17).

We observed a continuous, beaded, false network of varicose fibers, forming an epithelial plexus with few free nerve endings (35) as widely described in animals (14, 24, 31, 36) and humans (26). In contrast, we also noted PGP9.5-immunolabeled fibers in the epithelium, which formed arboreal receptive fields, derived from deeper thicker nerve bundles, with beaded axons and terminal varicosities suggestive of free nerve endings. This latter form is concordant with early descriptions of some pulmonary fibers (29) but it is not clear whether these might be functionally separate fibers. The pattern of neurofilament immunopositivity within the nerve trunks and smaller-diameter neurofilament-positive epithelial fibers are reminiscent of nonmyelinated terminals of myelinated afferents, which have been described in other mammals (37).

Only one notable study has previously observed PNECs in human whole mounts (26). Similar to that study, we observed a nonhomogenous distribution of PNECs with density measurement correlating to the upper range of that previously described. We cannot rule out that a disease process may increase PNEC numbers in our patients (38) but our estimation (0.2–1.2%) is consistent with other published work (39). Electron (40) and confocal (41) microscopic studies in animals have shown specialized epithelial cells together with nerves. Accordingly, it is probable that at least a proportion of these cells are innervated by vagal afferents (42). Although the formation of cytoneural junctions is generally regarded as unlikely, the close association of fibers with epithelial cells is strongly suggestive of the presence of afferent signaling (43). The chemical mediator for signaling between PNECs and vagal afferents is not known but may be ATP (43–45), which would be consistent with recent clinical studies of cough (46). The PGP9.5-immunonegative fibers we observed had fiber diameters that suggest they are A delta fibers and, despite the widely held belief that PGP9.5 is a panneuronal marker, some unpublished observations demonstrate PGP9.5-immunonegative nerves in human nodose ganglia (A. Myers, private communication).

Even where mechanoreceptors can be demonstrated in animals, such nerve endings are rarely identified by PGP9.5 (15, 31). Yet, where neurofilament antibodies have been used, they are easily identified (47) and highly abundant (13), strongly suggesting that such fibers are PGP9.5 negative. This may explain the absence of any previous descriptions of these structures in human tissue. These specialized receptors are difficult to identify even in rodent tissue where some of them do express PGP9.5 (28). Because these structures are PGP9.5 immunonegative, and on the whole neurofilaments are restricted to major branches, some additional unseen elements of these structures may remain to be elucidated. Nevertheless, we believe that the neurofilament-positive neurons we have identified are likely to represent the human equivalents of animal cough receptors, smooth muscle–associated airway receptor, and to some degree, NEB innervation (48).

Conclusions

Very few previous observations of airway innervation have been made in whole-mount biopsy tissue and as a result an incomplete picture of human airway innervation remains. However, using this technique we have provided several novel insights into the neuronal structures present in human endobronchial specimens. It is clear that the use of fresh tissue and diverse antibody techniques are very important to the accurate analysis of fiber location and morphometry. ■

Author disclosures are available with the text of this article at www.atsjournals.org.

Acknowledgment: The authors thank Dr. Allen Myers at Johns Hopkins University for his helpful discussions and guidance on immunostaining and microscopy. The Manchester Bioimaging Facility microscope used in this study was purchased with grants from BBSRC, Wellcome Trust, and the University of Manchester Strategic Fund. They also thank Roger Meadows for help with confocal microscopy. Equipment and samples used in this study were also funded by the National Institute of Health Research, Respiratory and Allergy Clinical Research Facility.

References

1. Canning BJ, Woo A, Mazzone SB. Neuronal modulation of airway and vascular tone and their influence on nonspecific airways responsiveness in asthma. *J Allergy (Cairo)* 2012;2012:108149.
2. Voll-Aanerud M, Eagan TML, Plana E, Omenaas ER, Bakke PS, Svanes C, Siroux V, Pin I, Antó JM, Leynaert B. Respiratory symptoms in adults are related to impaired quality of life, regardless of asthma and COPD: results from the European community respiratory health survey. *Health Qual Life Outcomes* 2010;8:107.
3. Irwin RS, Baumann MH, Bolser DC, Boulet LP, Braman SS, Brightling CE, Brown KK, Canning BJ, Chang AB, Dicpinigaitis PV, *et al*.; American College of Chest Physicians (ACCP). Diagnosis and management of cough executive summary: ACCP evidence-based clinical practice guidelines. *Chest* 2006; 129(1, Suppl)1S–23S.
4. Prudon B, Birring SS, Vara DD, Hall AP, Thompson JP, Pavord ID. Cough and glottic-stop reflex sensitivity in health and disease. *Chest* 2005; 127:550–557.
5. Groneberg DA, Niimi A, Dinh QT, Cosio B, Hew M, Fischer A, Chung KF. Increased expression of transient receptor potential vanilloid-1 in airway nerves of chronic cough. *Am J Respir Crit Care Med* 2004;170: 1276–1280.
6. Undem BJ, Chuaychoo B, Lee M-GG, Weinreich D, Myers AC, Kollarik M. Subtypes of vagal afferent C-fibres in guinea-pig lungs. *J Physiol* 2004;556:905–917.
7. Sampson SR, Vidruk EH. Properties of 'irritant' receptors in canine lung. *Respir Physiol* 1975;25:9–22.
8. Canning BJ, Mazzone SB, Meeker SN, Mori N, Reynolds SM, Undem BJ. Identification of the tracheal and laryngeal afferent neurones mediating cough in anaesthetized guinea-pigs. *J Physiol* 2004;557: 543–558.
9. Sant'Ambrogio G. Information arising from the tracheobronchial tree of mammals. *Physiol Rev* 1982;62:531–569.
10. Mazzone SB, Reynolds SM, Mori N, Kollarik M, Farmer DG, Myers AC, Canning BJ. Selective expression of a sodium pump isozyme by cough receptors and evidence for its essential role in regulating cough. *J Neurosci* 2009;29:13662–13671.
11. Brouns I, Pintelon I, De Proost I, Alewaters R, Timmermans JP, Adriaensen D. Neurochemical characterisation of sensory receptors in airway smooth muscle: comparison with pulmonary neuroepithelial bodies. *Histochem Cell Biol* 2006;125:351–367.
12. Canning BJ, Chang AB, Bolser DC, Smith JA, Mazzone SB, McGarvey L; CHEST Expert Cough Panel; CHEST Expert Cough Panel. Anatomy and neurophysiology of cough: CHEST Guideline and Expert Panel report. *Chest* 2014;146:1633–1648.
13. Yamamoto Y, Atoji Y, Suzuki Y. Nerve endings in bronchi of the dog that react with antibodies against neurofilament protein. *J Anat* 1995; 187:59–65.
14. Lamb JP, Sparrow MP. Three-dimensional mapping of sensory innervation with substance p in porcine bronchial mucosa: comparison with human airways. *Am J Respir Crit Care Med* 2002; 166:1269–1281.
15. Kusindarta DL, Atoji Y, Yamamoto Y. Nerve plexuses in the trachea and extrapulmonary bronchi of the rat. *Arch Histol Cytol* 2004;67:41–55.
16. Goldie RG, Fernandes L, Rigby P. Airway nerves: detection and visualisation. *Curr Opin Pharmacol* 2002;2:273–277.
17. Scott GD, Fryer AD, Jacoby DB. Quantifying nerve architecture in murine and human airways using three-dimensional computational mapping. *Am J Respir Cell Mol Biol* 2013;48:10–16.
18. O'Connell F, Springall DR, Moradoghli-Haftvani A, Krausz T, Price D, Fuller RW, Polak JM, Pride NB. Abnormal intraepithelial airway nerves in persistent unexplained cough? *Am J Respir Crit Care Med* 1995;152:2068–2075.
19. West P, Canning B, Hilton E, Khalid S, Holt K, Abdulqawi R, Woodcock A, Smith J. P155 visualisation of airway nerves in chronic cough: towards the identification of the human "cough receptor." *Thorax* 2012;67:A129–A130.
20. West P, Canning B, Woodcock A, Smith J. Whole-mount preparation and immunofluorescent observations of airway neuronal structures in chronic cough. Presented at the British Neuroscience Association 22nd National Biennial Meeting. April 7–10, 2013, London.
21. Hunter DD, Undem BJ. Identification and substance P content of vagal afferent neurons innervating the epithelium of the guinea pig trachea. *Am J Respir Crit Care Med* 1999;159:1943–1948.
22. Duarte AG, Terminella L, Smith JT, Myers AC, Campbell G, Lick S. Restoration of cough reflex in lung transplant recipients. *Chest* 2008; 134:310–316.
23. Arvidsson U, Riedl M, Elde R, Meister B. Vesicular acetylcholine transporter (VAChT) protein: a novel and unique marker for cholinergic neurons in the central and peripheral nervous systems. *J Comp Neurol* 1997;378:454–467.
24. Terada M, Iwanaga T, Takahashi-Iwanaga H, Adachi I, Arakawa M, Fujita T. Calcitonin gene-related peptide (CGRP)-immunoreactive nerves in the tracheal epithelium of rats: an immunohistochemical study by means of whole mount preparations. *Arch Histol Cytol* 1992;55:219–233.
25. Kummer W, Fischer A, Kurkowski R, Heym C. The sensory and sympathetic innervation of guinea-pig lung and trachea as studied by retrograde neuronal tracing and double-labelling immunohistochemistry. *Neuroscience* 1992;49:715–737.
26. Weichselbaum M, Sparrow MP, Hamilton EJ, Thompson PJ, Knight DA. A confocal microscopic study of solitary pulmonary neuroendocrine cells in human airway epithelium. *Respir Res* 2005;6:115.
27. Mazzone SB, Mori N, Canning BJ. Synergistic interactions between airway afferent nerve subtypes regulating the cough reflex in guinea-pigs. *J Physiol* 2005;569:559–573.
28. De Proost I, Pintelon I, Brouns I, Timmermans J-P, Adriaensen D. Selective visualisation of sensory receptors in the smooth muscle layer of ex-vivo airway whole-mounts by styryl pyridinium dyes. *Cell Tissue Res* 2007;329:421–431.
29. Elftman AG. The afferent and parasympathetic innervation of the lungs and trachea of the dog. *Am J Anat* 1943;72:1–27.
30. Spencer H, Leof D. The innervation of the human lung. *J Anat* 1964;98: 599–609.
31. Yamamoto Y, Ootsuka T, Atoji Y, Suzuki Y. Morphological and quantitative study of the intrinsic nerve plexuses of the canine trachea as revealed by immunohistochemical staining of protein gene product 9.5. *Anat Rec* 1998;250:438–447.
32. Pérez Fontán JJ, Velloff CR. Labeling of vagal motoneurons and central afferents after injection of cholera toxin B into the airway lumen. *Am J Physiol Lung Cell Mol Physiol* 2001;280:L152–L164.
33. Myers AC. Transmission in autonomic ganglia. *Respir Physiol* 2001; 125:99–111.
34. Agostoni E, Chinnock JE, De Daly MB, Murray JG. Functional and histological studies of the vagus nerve and its branches to the heart, lungs and abdominal viscera in the cat. *J Physiol* 1957;135:182–205.
35. Larson SD, Schelegle ES, Hyde DM, Plopper CG. The three-dimensional distribution of nerves along the entire intrapulmonary airway tree of the adult rat and the anatomical relationship between nerves and neuroepithelial bodies. *Am J Respir Cell Mol Biol* 2003;28:592–599.
36. Watanabe N, Horie S, Michael GJ, Keir S, Spina D, Page CP, Priestley JV. Immunohistochemical co-localization of transient receptor potential vanilloid (TRPV)1 and sensory neuropeptides in the guinea-pig respiratory system. *Neuroscience* 2006;141:1533–1543.
37. Tsuda K, Maeyama T, Shin T. Ultrastructure of the myelinated nerve fibers in the feline laryngeal mucosa. *Acta Otolaryngol Suppl* 1998;539:95–97.
38. Pilmane M, Luts A, Sundler F. Changes in neuroendocrine elements in bronchial mucosa in chronic lung disease in adults. *Thorax* 1995;50: 551–554.
39. Boers JE, den Brok JL, Koudstaal J, Arends JW, Thunnissen FB. Number and proliferation of neuroendocrine cells in normal human airway epithelium. *Am J Respir Crit Care Med* 1996;154:758–763.
40. Luciano L, Reale E, Ruska H. On a "chemoreceptive" sensory cell in the tachea of the rat [in German]. *Z Zellforsch Mikrosk Anat* 1968;85: 350–375.
41. Krasteva G, Canning BJ, Hartmann P, Veres TZ, Papadakis T, Mühlfeld C, Schliecker K, Tallini YN, Braun A, Hackstein H, *et al*. Cholinergic chemosensory cells in the trachea regulate breathing. *Proc Natl Acad Sci USA* 2011;108:9478–9483.
42. Brouns I, De Proost I, Pintelon I, Timmermans JP, Adriaensen D. Sensory receptors in the airways: neurochemical coding of smooth muscle-associated airway receptors and pulmonary neuroepithelial body innervation. *Auton Neurosci* 2006;126-127:307–319.

43. Lembrechts R, Brouns I, Schnorbusch K, Pintelon I, Timmermans J-PP, Adriaensen D. Neuroepithelial bodies as mechanotransducers in the intrapulmonary airway epithelium: involvement of TRPC5. *Am J Respir Cell Mol Biol* 2012;47:315–323.
44. Weigand LA, Ford AP, Undem BJ. A role for ATP in bronchoconstriction-induced activation of guinea pig vagal intrapulmonary C-fibres. *J Physiol* 2012;590:4109–4120.
45. Saunders CJ, Reynolds SD, Finger TE. Chemosensory brush cells of the trachea. A stable population in a dynamic epithelium. *Am J Respir Cell Mol Biol* 2013;49:190–196.
46. Abdulqawi R, Dockry R, Holt K, Layton G, McCarthy BG, Ford AP, Smith JA. P2X3 receptor antagonist (AF-219) in refractory chronic cough: a randomised, double-blind, placebo-controlled phase 2 study. *Lancet* 2015;385:1198–1205.
47. Mazzone SB, McGovern AE. Immunohistochemical characterization of nodose cough receptor neurons projecting to the trachea of guinea pigs. *Cough* 2008;4:9.
48. Adriaensen D, Brouns I, Pintelon I, De Proost I, Timmermans JP. Evidence for a role of neuroepithelial bodies as complex airway sensors: comparison with smooth muscle-associated airway receptors. *J Appl Physiol (1985)* 2006;101:960–970.